

Simulation complexity of open quantum dynamics: Connection with tensor networks

I. A. Luchnikov,^{1,2} S. V. Vintskevich,^{2,3} H. Ouerdane,¹ and S. N. Filippov^{2,4,5}

¹Center for Energy Science and Technology, Skolkovo Institute of Science and Technology,
3 Nobel Street, Skolkovo, Moscow Region 121205, Russia

²Moscow Institute of Physics and Technology, Institutskii Per. 9, Dolgoprudny, Moscow Region 141700, Russia

³A.M. Prokhorov General Physics Institute, Russian Academy of Sciences, Moscow, Russia

⁴Valiev Institute of Physics and Technology of Russian Academy of Sciences, Nakhimovskii Pr. 34, Moscow 117218, Russia

⁵Steklov Mathematical Institute of Russian Academy of Sciences, Gubkina St. 8, Moscow 119991, Russia

The difficulty to simulate the dynamics of open quantum systems resides in their coupling to many-body reservoirs with exponentially large Hilbert space. Applying a tensor network approach in the time domain, we demonstrate that effective small reservoirs can be defined and used for modeling open quantum dynamics. The key element of our technique is the timeline reservoir network (TRN), which contains all the information on the reservoir's characteristics, in particular, the memory effects timescale. The TRN has a one-dimensional tensor network structure, which can be effectively approximated in full analogy with the matrix product approximation of spin-chain states. We derive the sufficient bond dimension in the approximated TRN with a reduced set of physical parameters: coupling strength, reservoir correlation time, minimal timescale, and the system's number of degrees of freedom interacting with the environment. The bond dimension can be viewed as a measure of the open dynamics complexity. Simulation is based on the semigroup dynamics of the system and effective reservoir of finite dimension. We provide an illustrative example showing scope for new numerical and machine learning-based methods for open quantum systems.

PACS numbers: 02.10.Xm, 02.10.Yn, 03.65.Yz, 03.65.Aa, 03.65.Ca

Introduction. One of the most challenging and important problems of modern theoretical physics is the accurate simulation of an interacting many-body system. As the dimension of its Hilbert space grows exponentially with the system size, direct simulations become impossible. Exactly solvable models exist nonetheless [1]; they provide some insights into the properties of actual physical systems. Perturbation theory can be used only for problems that can be split into an exactly solvable part and a perturbative one provided that a relevant small parameter (e.g., weak interaction strength with respect to other energy scales) can be defined. For strongly interacting many-body systems, a range of techniques including, e.g., the Bethe ansatz [2], the dynamical mean field theory [3, 4], or the slave boson techniques [5, 6] have been developed and applied to problems like the diagonalization of the Kondo Hamiltonian or the Anderson impurity model [7–11]. Numerical approaches, which may significantly go beyond the range of applicability of analytical methods, have been also developed and proved quite successful, though they suffer from limits. For example, methods based on tensor networks [12–14] and the density matrix renormalization group [15–17] work well mainly for one-dimensional models. Quantum Monte Carlo (QMC) methods provide reliable ways to study the many-body problem [18], but for interacting fermion systems these approaches are plagued by the sign problem [19].

Unitary evolution of a many-body system is completely out of reach: dynamical versions of QMC calculations or efficient methods like the time-evolving block decimation algorithm cannot predict long-term time dynamics because of the Lieb-Robinson bound [20–23]. Having experimental access only to a part of a many-body system, one in fact deals with an *open* quantum dynamics of the subsystem (S), whereas the rest of the particles (modes)

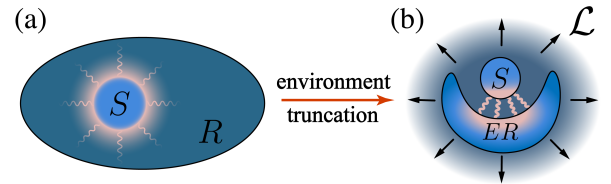


FIG. 1: Schematic of reservoir truncation.

play the role of environment also referred to as reservoir (R), see Fig. 1(a). The subsystem is described by a density operator $\rho_S(t) = \text{tr}_R[U(t)\rho(0)U^\dagger(t)]$, the evolution of which is still challenging to determine though the subsystem is relatively small compared to the environment [24, 25]: the partial trace, tr_R , disregards the environment degrees of freedom but $\rho(0)$ is the initial state of the *whole* many-body system and its evolution operator is $U(t) = e^{-itH}$. There exist particular exactly solvable models of open quantum dynamics [26–28]; however, without the Markov approximation the problem of open dynamics is typically impossible to solve directly because of the exponentially large dimension of the reservoir's Hilbert space [25, 29, 30]. Examples of complex open dynamics in structured reservoirs, where it is necessary to go beyond the Markov approximation, are presented in [31–42]. Therefore, new, numerically tractable approaches permitting significant progress in the field of open quantum dynamics simulation are highly desirable, and their development constitutes a timely challenge, especially in the study of quantum control and dynamical decoupling [40–42], and quantum dynamics induced by many-body reservoirs [43–46].

In this work, we show that the actual infinite environment can be replaced by a *finite*-dimensional effective

tive reservoir (ER) in such a way that the aggregate “ $S + ER$ ” experiences semigroup dynamics, see Fig. 1(b). This approach resembles the idea of Markovian embedding of non-Markovian dynamics [47–50] and the pseudomode method [51–53]. Our main result is the estimation of the minimal (sufficient) dimension d_{ER} of the effective reservoir expressed through a reduced set of parameters. Knowledge of d_{ER} enables one to efficiently simulate the complex dynamics of a subsystem of dimension d_S via $\rho_S(t) = \text{tr}_{ER}[e^{\mathcal{L}t}\rho_{S+ER}(0)]$, where the Gorini-Kossakowski-Sudarshan-Lindblad (GKSL) generator \mathcal{L} [54, 55] is easy to parameterize in this case: \mathcal{L} acts on $d_S d_{ER} \times d_S d_{ER}$ matrices and can be numerically found via machine learning techniques provided a sequence of measurements on the subsystem is performed [56]. Another machine learning algorithm [57] estimates d_{ER} within the training range $d_{ER} = 1, 2, 8, 16$ based on interventions in the open qubit evolution at 4 time moments.

Open quantum systems properties. Let \mathcal{H}_S and \mathcal{H}_R be Hilbert spaces of the subsystem and the reservoir, respectively. Typically $\dim(\mathcal{H}_S) \ll \dim(\mathcal{H}_R)$ as \mathcal{H}_S could be associated with, e.g., a qubit or other small system, and \mathcal{H}_R with a many-body quantum environment of a huge dimension. The total Hilbert space is $\mathcal{H} = \mathcal{H}_S \otimes \mathcal{H}_R$. As the environment is assumed to be in the thermodynamic limit, the dynamics of $\rho_S(t)$ is irreversible, i.e. the Poincaré recurrence time is infinite. When the subsystem and reservoir exchange energy, thermalization is expected on a long timescale [58], though the dynamics can be strongly non-Markovian at finite times [59].

The total Hamiltonian reads $H = H_0 + H_{\text{int}}$, where $H_0 = H_S \otimes \mathbb{1} + \mathbb{1} \otimes H_R$ involves individual Hamiltonians of the subsystem and the reservoir, $H_{\text{int}} = \gamma \sum_{i=1}^n A_i \otimes B_i$ is the interaction part with characteristic interaction strength γ ; n is the effective subsystem’s number of degrees of freedom interacting with the reservoir. Denote $B_i(t) = U^\dagger(t) B_i U(t)$, then $g_{ij}(t, t-s) = \text{tr}[B_i^\dagger(t) B_j(t-s) \rho(0)] - \text{tr}[B_i^\dagger(t) \rho(0)] \text{tr}[B_j(t-s) \rho(0)]$ is the reservoir correlation function [60]. Suppose $g_{ij}(t, t-s)$ decays exponentially with the growth of s over a characteristic time s_{ij} (see examples in [61, 62]), then $T = \max_{ij} s_{ij}$ is the reservoir correlation time. Suppose the Fourier transform of the reservoir correlation function decays significantly at the characteristic frequency Ω_{ij} , then $\tau = (\max_{ij} \Omega_{ij})^{-1}$ defines the minimal time scale in the dynamics. In the case of bosonic bath, $\tau = \omega_c^{-1}$, where ω_c is the cutoff frequency of the spectral function [63]. Our approach to determine the dimension d_{ER} of truncated environment is based on tensor network formalism in time domain, where the building blocks are responsible for evolution during time τ and the ancillary space is capable of transferring temporal correlations for the period T . Therefore, d_{ER} depends only on the following few physical parameters: γ , n , τ , and T .

Tensor network representation of open quantum dynamics. For simplicity, we resort to the vector representation

of a density operator:

$$\rho = \sum_{jk} \rho_{jk} |j\rangle \langle k| \rightarrow |\rho\rangle = \sum_{jk} \rho_{jk} |j\rangle \otimes |k\rangle, \quad (1)$$

which implies $Q\rho P \rightarrow Q \otimes P^T |\rho\rangle$. The dynamics of the whole system reads

$$|\rho(t)\rangle = \exp[-itH] \otimes \exp[itH^T] |\rho(0)\rangle. \quad (2)$$

The initial state $\rho(0)$ can be correlated in general, i.e. $\rho(0) = \sum_l \sigma_S^{(l)} \otimes \sigma_R^{(l)}$. The subsystem state $\rho_S(t) = \text{tr}_R \rho(t)$ in terms of vectors reads $|\rho_S(t)\rangle = \langle\psi_+| |\rho(t)\rangle$, where $\langle\psi_+| = \sum_{j=1}^{d_R} \mathbb{1}_S \otimes |j\rangle \otimes \mathbb{1}_S \otimes \langle j|$. For further convenience we introduce a new order of Hilbert spaces: $\mathcal{H}_S \otimes \mathcal{H}_R \otimes \mathcal{H}_S^\dagger \otimes \mathcal{H}_R^\dagger \rightarrow \mathcal{H}_S \otimes \mathcal{H}_S^\dagger \otimes \mathcal{H}_R \otimes \mathcal{H}_R^\dagger$.

The minimal timescale τ is a time step in discretized evolution; τ can always be reduced in such a way that $\gamma\tau \ll 1$, which permits application of the Trotter decomposition [64]. Note that we do not restrict our framework to a weak coupling between a subsystem and reservoir ($\gamma \ll \|H_0\|$); we rather adjust the minimal timescale τ in accordance with the interaction strength, which yields

$$|\rho(t)\rangle = \underbrace{\Phi_0(\tau) \Phi_{\text{int}}(\tau) \cdots \Phi_0(\tau) \Phi_{\text{int}}(\tau)}_{t/\tau \text{ times}} |\rho(0)\rangle + O(\gamma\tau), \quad (3)$$

where $\Phi_0(\tau)$ and $\Phi_{\text{int}}(\tau)$ are responsible for the noninteractive and interactive evolutions of the subsystem and environment:

$$\Phi_0(\tau) = \exp[-i\tau H_S] \otimes \exp[i\tau H_S^T] \otimes \exp[-i\tau H_R] \otimes \exp[i\tau H_R^T], \quad (4)$$

$$\Phi_{\text{int}}(\tau) = \sum_{i=0}^{2n} \mathcal{A}_i(\tau) \otimes \mathcal{B}_i(\tau), \quad (5)$$

$$\mathcal{A}_i(\tau) = \begin{cases} \mathbb{1} \otimes \mathbb{1} & \text{if } i = 0, \\ \sqrt{\gamma\tau} A_i \otimes \mathbb{1} & \text{if } 1 \leq i \leq n, \\ \sqrt{\gamma\tau} \mathbb{1} \otimes A_{i-n}^T & \text{if } i \geq n+1, \end{cases} \quad (6)$$

$$\mathcal{B}_i(\tau) = \begin{cases} \mathbb{1} \otimes \mathbb{1} & \text{if } i = 0, \\ -i\sqrt{\gamma\tau} B_i \otimes \mathbb{1} & \text{if } 1 \leq i \leq n, \\ i\sqrt{\gamma\tau} \mathbb{1} \otimes B_{i-n}^T & \text{if } i \geq n+1. \end{cases} \quad (7)$$

The tensor network representation to calculate $|\rho_S(t)\rangle$ is presented in Fig. 2. It is a particular case of the general quantum circuits [65–69]. Each building block with m arms corresponds to a tensor of rank m . Connecting links denote contractions over the same indices. The vector $|\rho(t)\rangle$ has two multi-indices $j = (j_S, j_R)$ and $k = (k_S, k_R)$, so it is represented as a tensor of rank 4. The upper (bottom) row corresponds to the degrees of freedom of subsystem S (reservoir R). The operator $\Phi_0(\tau)$ is depicted by solid squares. The dashed squares with a link between them denote the operator $\Phi_{\text{int}}(\tau)$, with the link being responsible for summation $\sum_{i=0}^{2n}$ in formula (5). Concatenation with the building block ψ_+ in right bottom of Fig. 2 corresponds to the partial trace over R and will be further denoted by connecting link \supset .

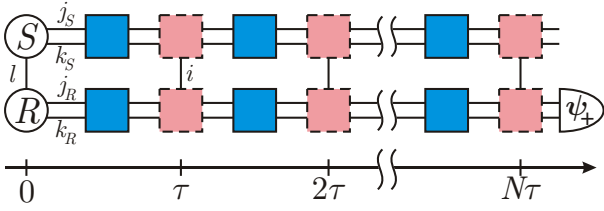


FIG. 2: Tensor network for open system dynamics.

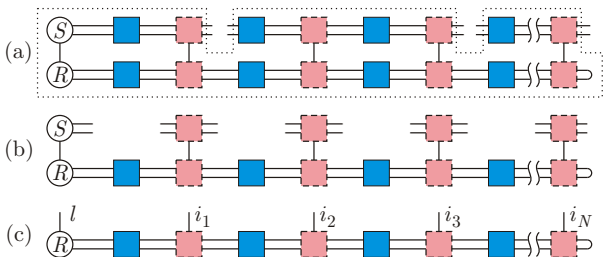
A key object in our study is the tensor in Fig. 3(c), which we call a *timeline reservoir network* (TRN). The TRN contains all the information on the reservoir and controls all features of open dynamics, including dissipation, Lamb shift, memory effects like revivals [25]. From the computational viewpoint, for a fixed time t , TRN is a tensor with t/τ indices. Since the physical reservoir has a finite memory depth T , the considered tensor must have vanishing correlations between apart indices. Tensors of such a type can be effectively approximated by one-dimensional tensor networks of matrix-product (MP) form.

The TRN is closely related to the recent reformulations of the Feynman-Vernon path integrals [63, 70–73] and the process tensor [68, 74–76], see Figs. 3(a)–3(b). In fact, the influence functional in Fig. 3(b) can be explicitly calculated in the case of a bosonic bath linearly coupled to the system [77] but it remains difficult to contract with the system initial state and unitary evolution tensors, so in Refs. [70–72] the contraction calculation is approximated by fixing a finite memory depth $K = T/\tau$. References [63, 73] further use MP approximation of the influence functional (with rank λ_{\max} and accuracy λ_c), which allows to deal with longer memory depths. Since λ_{\max} is d_{ER}^2 in our model, we actually estimate the complexity (λ_{\max}) of the algorithm in Ref. [63].

MP approximation of the TRN. From a mathematical viewpoint, the constructed TRN can be treated as a pure multipartite quantum state $|\psi\rangle$, where summation index $i_m = 0, \dots, 2n$ at time moment $t_m = m\tau$ plays the role of the physical index assigned to the m th particle:

$$|\psi\rangle = \sum_{l, i_1, i_2, \dots, i_N} \psi_{li_1 i_2 \dots i_N} |l\rangle \otimes |i_1\rangle \otimes |i_2\rangle \otimes \dots \otimes |i_N\rangle. \quad (8)$$

The only difference between the TRN and $|\psi\rangle$ is the nor-

FIG. 3: (a) Process tensor $\mathcal{T}(t_1; t_3; t_n)$ [68, 74–76]. (b) Influence functional [63, 70–73]. (c) Timeline reservoir network.

MP approximation of states	MP approximation of TRN
position of m 'th particle in space	time moment $t_m = m\tau$ on timeline
dimension of a particle's Hilbert space	twice the number of subsystem's degrees of freedom plus one, $2n + 1$
rank, bond dimension r (dimension of ancillary space)	square of dimension of effective reservoir, d_{ER}^2
correlation length, L	reservoir correlation time, T

TABLE I: Correspondence between physical descriptions of pure quantum states and TRN in MP approximation.

malization: $\text{TRN} \propto |\psi\rangle$, $\langle\psi|\psi\rangle = 1$.

A multipartite quantum state $|\psi\rangle$ with a finite correlation length L can be effectively described via MP approximation [12]. The benefit of such an approximation is that it is able to reproduce spatial correlations among particles within the characteristic length L . The effectiveness of approximation means that the bond dimension r of the ancillary space (rank of MP state) is rather small. Similarly, the TRN is able to effectively reproduce temporal correlations within the period T with a rather small dimension d_{ER} of effective reservoir. Since we deal with matrices, d_{ER}^2 is equivalent to the rank of corresponding MP state. The dimension of the physical space in the MP state is $2n + 1$, where n is the number of the subsystem's degrees of freedom involved in the interaction with environment. Note that $n \leq d_S^2$. The physics of MP approximations for states and TRN is summarized in Table I.

Suppose $|\psi^{(r)}\rangle$ is a rank- r MP approximation of the pure state $|\psi\rangle$. The approximation error $\epsilon(r)$ equals the Frobenius distance between $|\psi^{(r)}\rangle$ and $|\psi\rangle$. Consider $|\psi\rangle$ as a bipartite state, with parties being separated by a cut between the m th and $(m + 1)$ th particles. MP approximation effectively disregards low-weight contributions in the Schmidt decomposition of $|\psi\rangle$ with respect to such a cut. The approximation error $\epsilon(r)$ is related to the Rényi entropy of order α ($0 < \alpha < 1$), S_α of a single reduced density operator as follows [78]:

$$\ln[\epsilon(r)] \leq \frac{1-\alpha}{\alpha} \left[S_\alpha - \ln \left(\frac{r}{1-\alpha} \right) \right], \quad (9)$$

from which one readily obtains the sufficient bond dimension guaranteeing the arbitrary desired accuracy ϵ :

$$r_{\text{suff}}(\epsilon) = \min_{0 < \alpha < 1} (1 - \alpha) \epsilon^{-\alpha/(1-\alpha)} \exp(S_\alpha). \quad (10)$$

In the language of TRN, the sufficient rank is the square of minimal dimension of effective reservoir, d_{ER}^2 , which can reproduce all temporal correlations with error ϵ . Therefore, to find d_{ER} one needs to estimate the Rényi entropy S_α of tensor in Fig. 4 considered as a matrix M with 2 multi-indices (l, i_1, \dots, i_m) and (l', i'_1, \dots, i'_m) :

$$M_{(l, i_1, \dots, i_m), (l', i'_1, \dots, i'_m)} = \sum_{i_{m+1}, \dots, i_N} \psi_{l, i_1, \dots, i_m, i_{m+1}, \dots, i_N} \psi_{l', i'_1, \dots, i'_m, i_{m+1}, \dots, i_N}^* \quad (11)$$

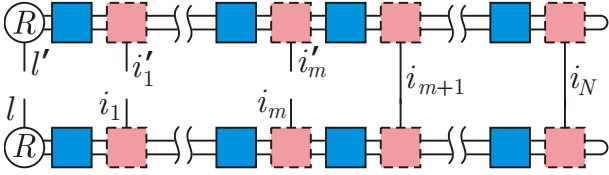


FIG. 4: Reduced matrix of TRN.

The Rényi entropy reads [79]:

$$S_\alpha \lesssim \frac{1}{1-\alpha} \ln \frac{[1 + 2n(\gamma\tau)^\alpha]^{T/\tau}}{(1 + 2n\gamma\tau)^{\alpha T/\tau}} \approx 2n\gamma T \frac{(\gamma\tau)^{\alpha-1} - \alpha}{1-\alpha}. \quad (12)$$

The entropy S_α is a measure of the time correlations in TRN. Substituting (12) in (10), we obtain the sufficient rank r_{suff} of MP approximation of TRN with desired physical properties (parameters γ , n , T , τ) and accuracy ϵ . On the other hand, the rank of MP approximation is the square of the dimension d_{ER} of the *effective* reservoir that can reproduce all the features of open dynamics (including memory effects) with accuracy ϵ . Therefore, it is possible to simulate the complex open system dynamics by using the effective reservoir of dimension

$$d_{ER}(\epsilon) = \min_{0 < \alpha < 1} \frac{\sqrt{1-\alpha}}{\epsilon^{\alpha/2(1-\alpha)}} \exp \left[n\gamma T \frac{(\gamma\tau)^{\alpha-1} - \alpha}{1-\alpha} \right]. \quad (13)$$

Once the effective reservoir is constructed, the aggregate “ $S + ER$ ” experiences the semigroup dynamics. This follows from the tensor network representation in Fig. 2. The TRN has a homogeneous structure and so does its MP approximation. The regular structure of building blocks in the time scale means that the same transformation $\mathbb{1} + \tau\mathcal{L}$ acts on “ $S + ER$ ” between the successive times $m\tau$ and $(m+1)\tau$. The GKSL generator \mathcal{L} [54, 55] acts on $d_S d_{ER} \times d_S d_{ER}$ density matrices and guarantees complete positivity of evolution.

Discussion. Although the actual environment consists of infinitely many modes, the developed theory facilitates the simulation of complex open system dynamics with a finite dimensional effective reservoir. The sufficient dimension d_{ER} depends on two combinations of physical parameters: $n\gamma T$ and $\gamma\tau$. Figure 5 shows that one can simulate the open dynamics on a classical computer for a wide range of parameters: $n\gamma T$ and $\gamma\tau$, accounting for all potential initial correlations between the system and its environment.

The first illustrative example is a decay of the two-level system (qubit) in multimode environment [79]. We compare the exactly solvable qubit dynamics, the Markov approximation ($d'_{ER} = 1$), and the approximation obtained with the reservoir of fixed dimension ($d''_{ER} = 2$). Figure 6 shows that the best Markovian approximation cannot reproduce oscillations in the exact dynamics, whereas the approximation with the fixed dimension $d''_{ER} = 2$ fits well the exact dynamics when the simulation complexity $d_{ER} \sim d''_{ER}$. However, if d_{ER} is several orders of magnitude larger than d''_{ER} , then the approximation is not able

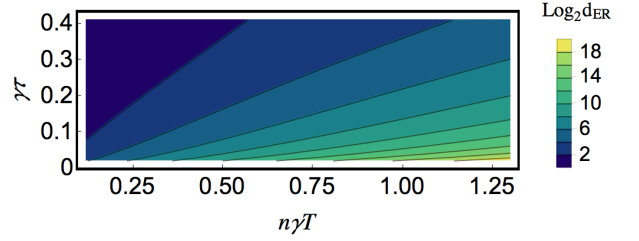


FIG. 5: Number of qubits $\log_2(d_{ER})$ in effective reservoir, which is sufficient for simulation of open dynamics with accuracy $\epsilon = 0.05$. $n\gamma T$ is dimensionless memory time and $\gamma\tau$ is dimensionless minimal timescale.

to reproduce memory effects present in the exact solution. Thus, d_{ER} does quantify the complexity of dynamics.

The second example is the double quantum dot charge qubit coupled to piezoelectric acoustic phonons [62]. Here, $n = 1$, $T \approx 4\tau$, $\tau = \omega_c^{-1}$, $\gamma = 0.05\omega_c$, and $\omega_c = 83$ GHz is the cutoff frequency of the spectral function. Eq. (13) yields $\log_2 d_{ER} = 4$ for $\epsilon = 0.05$, i.e. the non-Markovian qubit dynamics can be embedded into a Markovian evolution of the very qubit and 4 auxiliary ones.

The third example is the non-Markovian evolution of the qubit due to interaction with the dissipative pseudo-mode [52, 53]: $\frac{d\rho}{dt} = -i[H_0, \rho] + \Gamma(a\rho a^\dagger - \frac{1}{2}\{a^\dagger a, \rho\})$, where $H_0 = \omega_0 \sigma_+ \sigma_- + \omega a^\dagger a + \Omega_0 \sigma_x (a^\dagger + a)$ and ρ is the density operator for the qubit and the pseudomode. Physical parameters are $n = 1$, $T = \Gamma^{-1}$, $\tau = \omega^{-1}$, $\gamma = \Omega_0 \sqrt{n_0 + 1}$, where n_0 is the effective number of photons in the pseudomode. Our result, Eq. (13), estimates where the pseudomode oscillator can be truncated (Fock states with number of photons less than d_{ER}) to reproduce the system dynamics with precision ϵ at any time despite the memory effects and the counter-rotating terms in H_0 . In this example, construction of the effective reservoir reduces to the subspace spanned by d_{ER} lowest energy states of the pseudomode because the particular dissipator forces the pseudomode to the ground state.

There are physical scenarios in which the structure of the effective reservoir follows from the model. For in-

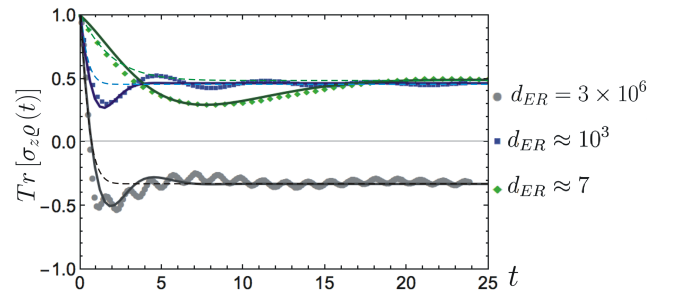


FIG. 6: Typical evolutions of parameter $\text{tr}[\sigma_z \rho(t)]$ of open qubit system $\rho(t)$ for different values of simulation complexity $d_{ER}(0.05)$ [79]. Dotted lines depict the exact dynamics. Dashed lines depict the best Markov approximations ($d'_{ER} = 1$). Solid lines are the approximations obtained with the reservoir of fixed dimension $d''_{ER} = 2$.

stance, in a nitrogen-vacancy center in diamond, the inherent nitrogen (^{14}N) nuclear spin ($I = 1$) serves as an effective reservoir for the electronic spin qubit [42]. In this case, $d_{ER} = 3$. Similarly, in a composite bipartite collision model [83], d_{ER} is given by the size of an ancillary system. In general, however, the structure of the effective reservoir is to be determined from the experimental data. Reference [56] proposes a machine learning algorithm to reconstruct the generator \mathcal{L} based on a series of repeated measurements on the open system.

Finally, our result is applicable to the influence functional tensor networks in Refs. [63, 73], where the analytical solution for open dynamics is not accessible, and provides the upper bound on the maximum bond dimension, $\lambda_{\max} < d_{ER}^2$. Conversely, for a fixed computationally tractable size of bond dimension, e.g., $\lambda_{\max} \sim 10^3$, our result provides the region of physical parameters $\gamma\tau$ and $n\gamma T$, for which the algorithm in Ref. [63] definitely works well.

Importantly, the TRN is a multidimensional tensor, so it can be approximated with MP form but also with other

constructions like multiscale entanglement renormalization ansatz [84, 85] or artificial neural networks [86, 87]. The benefit of such networks is that time correlations in the environment do not have to decay exponentially as for the MP approximation.

Conclusion. We gave a definition of simulation complexity of open quantum dynamics in terms of a reservoir's effective dimension. We showed that the tensor networks approach can be utilized to analyze memory effects in open dynamics. We provided an estimation of simulation complexity using a set of physical parameters. Our estimation is universal and fits well the arbitrary open quantum dynamics with finite memory.

Acknowledgments The authors thank Alexey Akimov, Mikhail Krechetov, Eugene Polyakov, Alexey Rubtsov, and Mario Ziman for fruitful discussions. The study is supported by Russian Foundation for Basic Research under Project No. 18-37-20073. I.A.L. thanks Russian Foundation for Basic Research for partial support under Project No. 18-37-00282.

Supplemental Material

Upper bound on Rényi entropy

Here we discuss the upper bound on Rényi entropy to clarify the derivation of formula (12) in the main text. Consider an arbitrary density matrix M that has the form $M = \sum_q \mathbf{v}_q \mathbf{v}_q^\dagger$, where the set of vectors $\{\mathbf{v}_q\}_q$ is not orthogonal nor normalized. Let us prove that the Rényi entropy $S_\alpha(M) = \frac{1}{1-\alpha} \ln \text{tr} M^\alpha$ satisfies the inequality $S_\alpha(M) \leq \frac{1}{1-\alpha} \ln \sum_q (\mathbf{v}_q^\dagger \mathbf{v}_q)^\alpha$ if $0 < \alpha < 1$.

In fact, the classical Rényi entropy H_α is Schur-concave for all $\alpha > 0$ (see, e.g., [80]), i.e. $H_\alpha(R) \leq H_\alpha(P)$ whenever the probability distribution P is majorized by the probability distribution R ($\sum_{i=1}^k P_i^\downarrow \leq \sum_{i=1}^k R_i^\downarrow$ for all $k = 1, 2, \dots$). By Theorem 10 of Ref. [81] the equality $M = \sum_q \mathbf{v}_q \mathbf{v}_q^\dagger$ implies that the distribution $V = \{\mathbf{v}_q^\dagger \mathbf{v}_q\}_q$ is majorized by the vector Λ of eigenvalues of M . Therefore,

$$S_\alpha(M) = H_\alpha(\Lambda) \leq H_\alpha(V) = \frac{1}{1-\alpha} \ln \sum_q (\mathbf{v}_q^\dagger \mathbf{v}_q)^\alpha. \quad (14)$$

Diagrammatic language for tensor networks

In this section we demonstrate key physical objects using tensor network representation (language).

Fig. 7(a) illustrates the timeline reservoir network (TRN) as an analogue of multipartite quantum state $|\psi\rangle$. It also depicts the TRN matrix in analogy with the density matrix $|\psi\rangle\langle\psi|$ for states.

In Fig. 7(b) we simplify the notation and coarse grain the elements of the tensor network. We replace double lines by single thick lines. The tracing element in the right hand side of network is depicted as a semicircle.

Fig. 7(c) depicts TRN matrix in terms of new notation.

In Fig. 7(d) we depict the reduced TRN matrix, which is constructed in analogy with the reduced density matrix ($\rho_s = \text{tr}_r \rho_{s+r}$). Connected indices between upper and lower parts of network mean summation, i.e. reduction over non-relevant part with time $t \geq m\tau$.

Given a reduced matrix M of TRN, namely,

$$M_{(l, i_1, \dots, i_m), (l', i'_1, \dots, i'_m)} = \sum_{i_{m+1}, \dots, i_N} \psi_{l, i_1, \dots, i_m, i_{m+1}, \dots, i_N} \psi_{l', i'_1, \dots, i'_m, i_{m+1}, \dots, i_N}^*. \quad (15)$$

one needs to estimate its Rényi entropy S_α . The result of section A is that $S_\alpha(M) \leq (1-\alpha)^{-1} \ln \sum_q (\mathbf{v}_q^\dagger \mathbf{v}_q)^\alpha$. In our

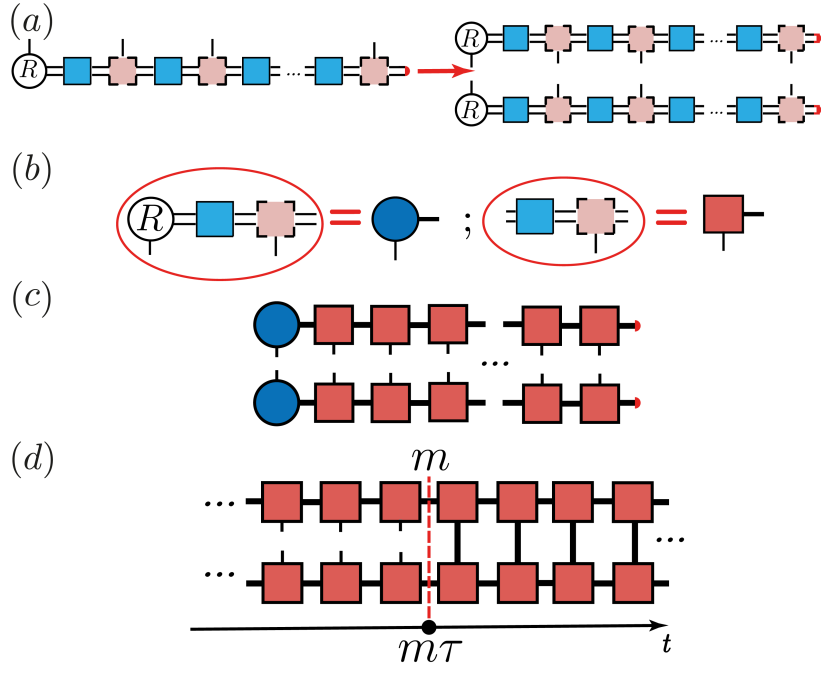


FIG. 7: (a) TRN and TRN matrix. (b) Change of notation to simplify tensor network representation. (c) TRN matrix in simplified notation. (d) Reduced matrix of TRN.

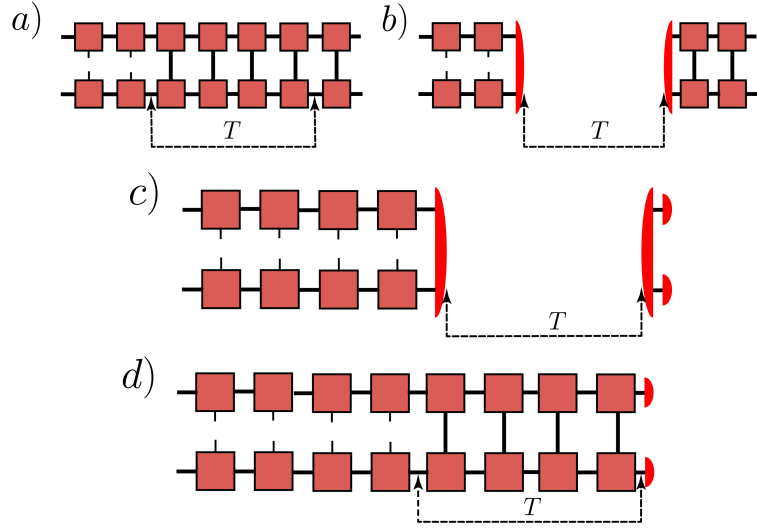


FIG. 8: (a) Reduced matrix of TRN and the reservoir correlation time T . (b) The absence of time correlations between blocks separated by time T . (c) The right hand side is a rank-0 tensor. (d) The marked tensor of length T is exactly the element \Rightarrow in Fig. 8(c).

$$S \leq - \sum_{i_1, \dots, i_{T/\tau}} \left[\begin{array}{ccccccc} \cdots & \text{red box} & \text{red box} & \text{red box} & \cdots & \text{red box} & \text{red arrow} \\ & | & | & | & & | & \\ & \text{red box} & \text{red box} & \text{red box} & \cdots & \text{red box} & \text{red arrow} \end{array} \right] \log \left[\begin{array}{ccccccc} \cdots & \text{red box} & \text{red box} & \text{red box} & \cdots & \text{red box} & \text{red arrow} \\ & | & | & | & & | & \\ & \text{red box} & \text{red box} & \text{red box} & \cdots & \text{red box} & \text{red arrow} \end{array} \right]$$

FIG. 9: Estimation of the von Neumann entropy of the reduced TRN within the framework of diagrammatic representation.

case $q = (i_{m+1}, \dots, i_N)$ and \mathbf{v}_q is a vector with components $\psi_{l, i_1, \dots, i_m, q}$, so we have

$$S_\alpha \leq (1 - \alpha)^{-1} \ln \sum_{i_{m+1}, \dots, i_N} \left(\sum_{l, i_1, \dots, i_m} |\psi_{l, i_1, \dots, i_m, i_{m+1}, \dots, i_N}|^2 \right)^\alpha. \quad (16)$$

Let us consider the physical structure of M , see Fig. 8. In Fig. 8(a), we explicitly mark out the reservoir correlation time T . Since temporal correlations decay within the time period T , we assume that time correlations between nodes separated by time $t \geq T$ can be neglected. This means that the action of tensor network of length T can be replaced by a simpler tensor of the form $\Rightarrow \Leftarrow$, see Fig. 8(b). Thus,

$$\Rightarrow \text{tensor of length } t \geq T \Leftarrow \iff \Rightarrow \Leftarrow. \quad (17)$$

Concatenation of the tensor \Leftarrow with the rest of right-hand side tensor is merely a number (rank-0 tensor), Fig. 8(c). In other words, the contribution of indexes $i_{m+T/\tau+1}, i_{m+T/\tau+2}, \dots, i_N$ in formula (16) is trivial: the summation over indexes $i_{m+T/\tau+1}, i_{m+T/\tau+2}, \dots, i_N$ does not change the structure of the matrix M as it only leads to a multiplication factor. The reduced matrix M of TRN is not affected by time moments happening after the reservoir correlation timescale has passed.

That observation explains the fact why in formula (16) one can replace the tensor $\psi_{l, i_1, \dots, i_m, i_{m+1}, \dots, i_N}$ by a tensor $\tilde{\psi}_{l, i_1, \dots, i_m, i_{m+1}, \dots, i_{m+T/\tau}}$ of finite length and appropriate normalization $\sum_{l, i_1, \dots, i_{m+T/\tau}} |\tilde{\psi}_{l, i_1, \dots, i_{m+T/\tau}}|^2 = 1$.

Therefore, the Rényi entropy of reduced TRN matrix equals the Rényi entropy of a tensor depicted in the left-hand side of Fig. 8(c). The element \Rightarrow in the left-hand side of Fig. 8(c) can be replaced by a tensor of finite length T , and we end up with a tensor network illustrated in Fig. 8(d). Following the notation of the main text,

$$\text{Fig. 8(d)} \iff \sum_{i_{m+1}, \dots, i_{m+T/\tau}} \tilde{\psi}_{l, i_1, \dots, i_m, i_{m+1}, \dots, i_{m+T/\tau}} \tilde{\psi}_{l', i'_1, \dots, i'_m, i_{m+1}, \dots, i_{m+T/\tau}}^*. \quad (18)$$

and we get

$$S_\alpha \lesssim (1 - \alpha)^{-1} \ln \sum_{i_{m+1}, \dots, i_{m+T/\tau}} \left(\sum_{l, i_1, \dots, i_m} |\tilde{\psi}_{l, i_1, \dots, i_m, i_{m+1}, \dots, i_{m+T/\tau}}|^2 \right)^\alpha. \quad (19)$$

Recalling the explicit structure of TRN given by formulas (5)–(7) in the main text, we find

$$\sum_{l, i_1, \dots, i_m} |\tilde{\psi}_{l, i_1, \dots, i_m, i_{m+1}, \dots, i_{m+T/\tau}}|^2 \approx (1 + 2n\gamma\tau)^{-T/\tau} \prod_{p=1}^{T/\tau} \begin{cases} 1, & i_{m+p} = 0, \\ \gamma\tau, & i_{m+p} = 1, \dots, 2n. \end{cases} \quad (20)$$

Substituting this result in (19), we obtain

$$S_\alpha \lesssim \frac{1}{1 - \alpha} \ln \frac{[1 + 2n(\gamma\tau)^\alpha]^{T/\tau}}{(1 + 2n\gamma\tau)^{\alpha T/\tau}} \approx 2n\gamma T \frac{(\gamma\tau)^{\alpha-1} - \alpha}{1 - \alpha}. \quad (21)$$

To finalize the explanation of diagrammatic language in the estimation of entropy S_α , in Fig. 9 we depict the case $\alpha \rightarrow 1$ when S_α tends to the von Neumann entropy.

Exactly solvable model

In this section, we consider a particular example of an exactly solvable open quantum dynamics. Let S be a two-level system with energy separation Ω and R be a bosonic bath at zero temperature. The total Hamiltonian reads (hereafter the Planck constant $\hbar = 1$)

$$H = \Omega\sigma_+\sigma_- + \sum_m \omega_m b_m^\dagger b_m + \sum_m g_m (b_m^\dagger \sigma_- + b_m \sigma_+), \quad (22)$$

where $\sigma_+ = |1\rangle\langle 0|$ and $\sigma_- = |0\rangle\langle 1|$, $|0\rangle$ and $|1\rangle$ are the ground and excited states of the two-level system, respectively, index m enumerates bosonic modes, b_m and b_m^\dagger are the annihilation and creation operators for bosons in m 'th mode, g_m is the coupling strength given by formula

$$g_m = \begin{cases} g & \text{if } \omega_{\min} \leq \omega_m \leq \omega_{\max}, \\ 0 & \text{otherwise.} \end{cases} \quad (23)$$

Consider the equidistant set of mode frequencies ω_m with $\omega_{m+1} - \omega_m = \Delta\omega$, then the bath consists of $N = \frac{\omega_{\max} - \omega_{\min}}{\Delta\omega}$ modes with frequencies $\omega_m = \omega_{\min} + m\Delta\omega$, $m = 1, \dots, N$.

The initial state of “ $S+R$ ” is pure and has the form

$$|\psi(0)\rangle = |1, \text{vac}\rangle, \quad (24)$$

which implies that the two-level system is in the excited state and that the bath has no excitation. The Hamiltonian (22) preserves the number of excitations, so the solution of the Schrödinger equation $i\frac{d}{dt}|\psi(t)\rangle = H|\psi(t)\rangle$ has the form

$$|\psi(t)\rangle = \alpha(t)|1, \text{vac}\rangle + \sum_m \beta_m(t)|0, 1_m\rangle, \quad (25)$$

where the coefficients $\alpha(t)$ and $\beta_m(t)$ satisfy the following system of differential equations

$$i\frac{d}{dt} \begin{bmatrix} \alpha(t) \\ \beta_1(t) \\ \beta_2(t) \\ \vdots \\ \beta_N(t) \end{bmatrix} = \begin{bmatrix} \Omega & g & g & \dots & g \\ g & \Delta\omega & 0 & \dots & 0 \\ g & 0 & 2\Delta\omega & \dots & 0 \\ \vdots & \vdots & \vdots & \ddots & \vdots \\ g & 0 & 0 & \dots & N\Delta\omega \end{bmatrix} \begin{bmatrix} \alpha(t) \\ \beta_1(t) \\ \beta_2(t) \\ \vdots \\ \beta_N(t) \end{bmatrix} \quad (26)$$

and meet the initial requirements $\alpha(0) = 1$ and $\beta_m(0) = 0$.

The parameter $\alpha(t)$ is a solution of:

$$\frac{d}{dt}\alpha(t) = -i\Omega\alpha(t) - \sum_{k=1}^N g^2 \int_0^t \exp[-ik\Delta\omega(t-t')] \alpha(t') dt'. \quad (27)$$

Assume $\Delta\omega \rightarrow 0$, we replace the summation \sum_k by the integration:

$$\sum_{k=1}^N \rightarrow \frac{1}{\Delta\omega} \int_{\omega_{\min}}^{\omega_{\max}} d\omega. \quad (28)$$

Therefore, we obtain the model with reservoir containing an infinite number of modes. Nonetheless, such a model is still solvable as the parameter $\alpha(t)$ is a solution of the following integrodifferential equation:

$$\frac{d}{dt}\alpha(t) = -i\Omega\alpha(t) - \frac{g^2}{\Delta\omega} \int_0^t G(t-t')\alpha(t')dt', \quad G(t-t') = \int_{\omega_{\min}}^{\omega_{\max}} \exp[-i\omega(t-t')] d\omega. \quad (29)$$

Formally $\alpha(t)$ reads

$$\alpha(t) = \frac{1}{2\pi i} \int_{-\infty+\epsilon}^{\infty+\epsilon} ds e^{st} \frac{1}{s + i\Omega + \frac{g^2}{\Delta\omega} \int_{\omega_{\min}}^{\omega_{\max}} d\omega \frac{1}{s+i\omega}}, \quad (30)$$

and the quantity $\text{tr}[\sigma_z \rho(t)]$ illustrated in Fig. 6 in the main text equals $\text{tr}[\sigma_z \rho(t)] = 2|\alpha(t)|^2 - 1$.

Now, let us define the parameters T , τ , γ , n needed for the estimation of simulation complexity (the dimension of effective reservoir, d_{ER}). The memory kernel G decays significantly within the reservoir correlation time T , which in our case equals $T = \frac{1}{\omega_{\max} - \omega_{\min}}$. The minimal timescale of evolution is $\tau = \frac{1}{\omega_{\max}}$. Comparing the general form of interaction Hamiltonian

$H_{\text{int}} = \gamma \sum_{i=1}^n A_i \otimes B_i$ and the interaction Hamiltonian in our example $g \sum_{m=1}^{\frac{\omega_{\max} - \omega_{\min}}{\Delta\omega}} (b_m^\dagger \sigma_- + b_m \sigma_+)$, we conclude that $n = 2$ and $\gamma = g \frac{\omega_{\max} - \omega_{\min}}{\Delta\omega}$. Fixing the accuracy $\epsilon = 0.05$ and substituting parameters T , τ , γ , n in formula (15) in the main text, we calculate the sufficient dimension of effective reservoir d_{ER} for three different evolutions depicted in Fig. 6 in the main text.

Semigroup evolution of system ($d'_{ER} = 1$)

Direct application of the weak-coupling and Born–Markov approximations [25] to the model in section C results in the exponential decay $\text{tr}[\sigma_+ \sigma_- \rho(t)] = \exp(-\Gamma t)$ because the reservoir is assumed to be time-independent (always in a vacuum state). Such a behavior is in strong contrast to the exact solution in Fig. 6 in the main text, where the steady state has a non-zero population $\text{tr}[\sigma_+ \sigma_- \rho(\infty)]$.

A general semigroup evolution of the very qubit corresponds to the situation, when one forcibly fixes the dimension $d'_{ER} = 1$.

Let us consider the semigroup evolution of the qubit with a GKSL generator, which takes into account the finite population of excited state:

$$\frac{d\rho}{dt} = -i\Omega[\sigma_+ \sigma_-, \rho] + \gamma_\downarrow \left(\sigma_- \rho \sigma_+ - \frac{1}{2} \{ \sigma_+ \sigma_-, \rho \} \right) + \gamma_\uparrow \left(\sigma_+ \rho \sigma_- - \frac{1}{2} \{ \sigma_- \sigma_+, \rho \} \right). \quad (31)$$

Note that this equation is nothing else but the generalized amplitude damping process [82]. Adjusting the relaxation rates γ_\downarrow and γ_\uparrow , we get the best Markov approximations shown in Fig. 6 in the main text. This figure also illustrates that the best Markov approximation cannot reproduce non-Markovian memory effects, the correct effective dimension d_{ER} being much greater than $d'_{ER} = 1$.

Semigroup evolution of system and reservoir of fixed dimension $d''_{ER} = 2$

Let us consider a model with the small reservoir of forcibly fixed dimension $d''_{ER} = 2$ such that the system and the small reservoir altogether experience the semigroup dynamics. Such a model would be a good approximation of the exact dynamics found in section C if the simulation complexity $d_{ER} \sim d''_{ER}$.

We consider the following parameterization of the GKSL generator \mathcal{L} governing the evolution equation $\frac{d\rho}{dt} = \mathcal{L}\rho$ for the density operator $\rho(t)$ of the two level system and small reservoir:

$$\begin{aligned} \mathcal{L}\rho(t) &= -i[h, \rho(t)] + \mathcal{D}(\rho(t)), \\ h &= \Omega_1 \sigma_+ \sigma_- \otimes \mathbb{1} + \Omega_2 \mathbb{1} \otimes \sigma_+ \sigma_- + \tilde{g}(\sigma_+ \otimes \sigma_- + \sigma_- \otimes \sigma_+), \\ \mathcal{D}(\rho(t)) &= \gamma_{1,\downarrow} \left(\sigma_- \otimes \mathbb{1} \rho(t) \sigma_+ \otimes \mathbb{1} - \frac{1}{2} \{ \sigma_+ \sigma_- \otimes \mathbb{1}, \rho(t) \} \right) \\ &\quad + \gamma_{1,\uparrow} \left(\sigma_+ \otimes \mathbb{1} \rho(t) \sigma_- \otimes \mathbb{1} - \frac{1}{2} \{ \sigma_- \sigma_+ \otimes \mathbb{1}, \rho(t) \} \right) \\ &\quad + \gamma_{2,\downarrow} \left(\mathbb{1} \otimes \sigma_- \rho(t) \mathbb{1} \otimes \sigma_+ - \frac{1}{2} \{ \mathbb{1} \otimes \sigma_+ \sigma_-, \rho(t) \} \right) \\ &\quad + \gamma_{2,\uparrow} \left(\mathbb{1} \otimes \sigma_+ \rho(t) \mathbb{1} \otimes \sigma_- - \frac{1}{2} \{ \mathbb{1} \otimes \sigma_- \sigma_+, \rho(t) \} \right). \end{aligned} \quad (32)$$

The parameter Ω_1 is the energy difference between excited and ground states of the system S with a potential contribution of the Lamb shift; Ω_2 is the energy separation between levels of the effective reservoir; \tilde{g} is the coupling constant; $\gamma_{1,\downarrow}$ and $\gamma_{1,\uparrow}$ are decay rates of the system; and $\gamma_{2,\downarrow}$ and $\gamma_{2,\uparrow}$ are decay rates of the effective reservoir. All these parameters are adjusted to approximate the exact dynamics described in section C.

Figure 6 in the main text shows that the simple model with reservoir of fixed dimension $d''_{ER} = 2$ adequately describes non-Markovian dynamics with simulation complexity $d_{ER}(0.05) \approx 7$. However, such a simple model fails to reproduce memory effects associated with dynamics for which $d_{ER}(0.05) \sim 10^3$. This fact justifies that in order to reproduce memory effects with simulation complexity d_{ER} one has to deal with a reservoir of comparable dimension.

-
- [1] B. Sutherland, *Beautiful Models: 70 Years of Exactly Solved Quantum Many-Body Problems* (World Scientific, 2004).
 - [2] H. Bethe, Z. Phys. A **71**, 205 (1931).
 - [3] A. Georges, G. Kotliar, W. Krauth, and M. J. Rozenberg, Rev. Mod. Phys. **68**, 13 (1996).
 - [4] G. Kotliar, S. Y. Savrasov, K. Haule, V. S. Oudovenko, O. Parcollet, and C. A. Marianetti, Rev. Mod. Phys. **78**, 865 (2006).
 - [5] S. E. Barnes, J. Phys. F: Metal Phys. **6**, 1375 (1976).
 - [6] G. Kotliar and A. E. Ruckenstein, Phys. Rev. Lett. **57**, 1362 (1986).
 - [7] N. Andrei, Phys. Rev. Lett. **45**, 379 (1980).
 - [8] P. B. Wiegmann, Phys. Lett. A **80**, 163 (1980).
 - [9] A. Georges and G. Kotliar, Phys. Rev. B **45**, 6479 (1992).
 - [10] R. Frésard, H. Ouerdane, and T. Kopp, Nucl. Phys. B **785**, 286 (2007).
 - [11] R. Frésard, H. Ouerdane, and T. Kopp, EPL **82**, 31001 (2008).
 - [12] R. Orús, Annals Phys. **349**, 117 (2014).
 - [13] R. Orús, Euro. Phys. J. B **87**, 280 (2014).
 - [14] F. Verstraete, V. Murg, and J. I. Cirac, Advances Phys. **57**, 143 (2008).
 - [15] S. R. White, Phys. Rev. Lett. **69**, 2863 (1992).
 - [16] U. Schollwöck, Annals Phys. **326**, 96 (2011).
 - [17] U. Schollwöck, Phil. Trans. Royal Soc. London A **369**, 2643 (2011).
 - [18] D. P. Landau and K. Binder, *A guide to Monte Carlo simulations in statistical physics* (Cambridge University Press, Cambridge, 2009).
 - [19] E. Y. Loh, Jr., J. E. Gubernatis, R. T. Scalettar, S. R. White, D. J. Scalapino, and R. L. Sugar, Phys. Rev. B **41**, 9301 (1990).
 - [20] E. Lieb and D. Robinson, Commun. Math. Phys. **28**, 251 (1972).
 - [21] U. Schollwöck, "DMRG: Ground states, time evolution, and spectral functions," Chap. 16 in *Emergent Phenomena in Correlated Matter* edited by E. Pavarini, E. Koch, and U. Schollwöck (Verlag des Forschungszentrum Jülich, 2013).
 - [22] T. Prosen and M. Žnidarič, Phys. Rev. E **75**, 015202(R) (2007).
 - [23] H.-T. Chen, G. Cohen, and D. R. Reichman, J. Chem. Phys. **146**, 054106 (2017).
 - [24] E. B. Davies, *Quantum Theory of Open Systems*, (Academic Press, London, 1976).
 - [25] H.-P. Breuer and F. Petruccione, *The Theory of Open Quantum Systems* (Oxford University Press, Oxford, 2002).
 - [26] J. Rau, Phys. Rev. **129**, 1880 (1963).
 - [27] G. M. Palma, K.-A. Suominen, and A. K. Ekert, Proc. R. Soc. London A **452**, 567 (1996).
 - [28] S. N. Filippov, J. Piilo, S. Maniscalco, and M. Ziman, Phys. Rev. A **96**, 032111 (2017).
 - [29] R. Alicki and K. Lendi, *Quantum Dynamical Semi-Groups and Applications*, Lecture Notes Physics **286** (Springer-Verlag, Berlin, 1987).
 - [30] A. S. Holevo, *Quantum systems, channels, information. A mathematical introduction* (de Gruyter, Berlin/Boston, 2012).
 - [31] B.-H. Liu, L. Li, Y.-F. Huang, C.-F. Li, G.-C. Guo, E.-M. Laine, H.-P. Breuer, and J. Piilo, Nat. Phys. **7**, 931 (2011).
 - [32] C. Navarrete-Benlloch, I. de Vega, D. Porras, and J. I. Cirac, New J. Phys. **13**, 023024 (2011).
 - [33] J. Ma, Z. Sun, X. Wang, and F. Nori, Phys. Rev. A **85**, 062323 (2012).

- [34] U. Hoeppe, C. Wolff, J. Küchenmeister, J. Niegemann, M. Drescher, H. Benner, and K. Busch, *Phys. Rev. Lett.* **108**, 043603 (2012).
- [35] W. L. Yang, J.-H. An, C. Zhang, M. Feng, and C. H. Oh, *Phys. Rev. A* **87**, 022312 (2013).
- [36] K. Roy-Choudhury and S. Hughes, *Optica* **2**, 434 (2015).
- [37] S. Gröblacher, A. Trubarov, N. Prigge, G. D. Cole, M. Aspelmeyer, and J. Eisert, *Nat. Commun.* **6**, 7606 (2015).
- [38] A. González-Tudela and J. I. Cirac, *Phys. Rev. Lett.* **119**, 143602 (2017).
- [39] M. Wittemer, G. Clos, H.-P. Breuer, U. Warring, and T. Schaetz, *Phys. Rev. A* **97**, 020102(R) (2018).
- [40] F. Wang, P.-Y. Hou, Y.-Y. Huang, W.-G. Zhang, X.-L. Ouyang, X. Wang, X.-Z. Huang, H.-L. Zhang, L. He, X.-Y. Chang, and L.-M. Duan, *Phys. Rev. B* **98**, 064306 (2018).
- [41] S. Peng, X. Xu, K. Xu, P. Huang, P. Wang, X. Kong, X. Rong, F. Shi, C. Duan, and J. Du, *Sci. Bull.* **63**, 336 (2018).
- [42] J. F. Haase, P. J. Vetter, T. Unden, A. Smirne, J. Rosskopf, B. Naydenov, A. Stacey, F. Jelezko, M. B. Plenio, and S. F. Huelga, *Phys. Rev. Lett.* **121**, 060401 (2018).
- [43] M. Žnidarič, C. Pineda, and I. García-Mata, *Phys. Rev. Lett.* **107**, 080404 (2011).
- [44] O. Viyuela, A. Rivas, and M. A. Martin-Delgado, *Phys. Rev. B* **86**, 155140 (2012).
- [45] R. Vasseur, S. A. Parameswaran, and J. E. Moore, *Phys. Rev. B* **91**, 140202(R) (2015).
- [46] U. Marzolino and T. Prosen, *Phys. Rev. B* **96**, 104402 (2017).
- [47] A. A. Budini, *Phys. Rev. A* **88**, 032115 (2013).
- [48] S. Xue, M. R. James, A. Shabani, V. Ugrinovskii, and I. R. Petersen, Quantum filter for a class of non-Markovian quantum systems, *54th IEEE Conference on Decision and Control (Osaka, Japan)* (2015), pp. 7096-7100.
- [49] S. Xue, T. Nguyen, M. R. James, A. Shabani, V. Ugrinovskii, and I. R. Petersen, Modelling and filtering for non-Markovian quantum systems, arXiv:1704.00986.
- [50] D. Tamascelli, A. Smirne, S. F. Huelga, and M. B. Plenio, *Phys. Rev. Lett.* **120**, 030402 (2018).
- [51] A. Imamoglu, *Phys. Rev. A* **50**, 3650 (1994).
- [52] B. M. Garraway, *Phys. Rev. A* **55**, 2290 (1997).
- [53] L. Mazzola, S. Maniscalco, J. Piilo, K.-A. Suominen, and B. M. Garraway, *Phys. Rev. A* **80**, 012104 (2009).
- [54] V. Gorini, A. Kossakowski, and E. C. G. Sudarshan, *J. Math. Phys. (N.Y.)* **17**, 821 (1976).
- [55] G. Lindblad, *Commun. Math. Phys.* **48**, 119 (1976).
- [56] I. A. Luchnikov, S. V. Vintskevich, D. A. Grigoriev, and S. N. Filippov, Machine learning of Markovian embedding for non-Markovian quantum dynamics, arXiv:1902.07019.
- [57] S. Shrapnel, F. Costa, and G. Milburn, *Int. J. of Quantum Inf.* **16**, 1840010 (2018).
- [58] R. Kosloff, *Entropy* **15**, 2100 (2013).
- [59] I. de Vega and D. Alonso, *Rev. Mod. Phys.* **89**, 015001 (2017).
- [60] H. F. Arnoldus and T. F. George, *J. Math. Phys. (N. Y.)* **28**, 2731 (1987).
- [61] U. Weiss, *Quantum Dissipative Systems*, 2nd ed. (World Scientific, Singapore, 1999).
- [62] M. Thorwart, J. Eckel, and E. R. Mucciolo, *Phys. Rev. B* **72**, 235320 (2005).
- [63] A. Strathearn, P. Kirton, D. Kilda, J. Keeling, and B. W. Lovett, *Nat. Commun.* **9**, 3322 (2018).
- [64] M. Suzuki, *J. Math. Phys.* **26**, 601 (1985).
- [65] G. Chiribella, G. M. D'Ariano, and P. Perinotti, *Phys. Rev. Lett.* **101**, 060401 (2008).
- [66] G. Chiribella, G. M. D'Ariano, and P. Perinotti, *Phys. Rev. A* **80**, 022339 (2009).
- [67] L. Hardy, *Phil. Trans. R. Soc. A* **370**, 3385 (2012).
- [68] S. Milz, F. A. Pollock, and K. Modi, *Open Syst. Inf. Dyn.* **24**, 1740016 (2017).
- [69] F. Costa and S. Shrapnel, *New J. Phys.* **18**, 063032 (2016).
- [70] N. Makri and D. E. Makarov, *J. Chem. Phys.* **102**, 4611 (1995).
- [71] E. Sim, *J. Chem. Phys.* **115**, 4450 (2001).
- [72] A. Strathearn, B. W. Lovett, and P. Kirton, *New J. Phys.* **19**, 093009 (2017).
- [73] M. R. Jørgensen and F. A. Pollock, Exploiting the causal tensor network structure of quantum processes to efficiently simulate non-Markovian path integrals, arXiv:1902.00315.
- [74] F. A. Pollock, C. Rodríguez-Rosario, T. Frauenheim, M. Paternostro, and K. Modi, *Phys. Rev. A* **97**, 012127 (2018).
- [75] F. A. Pollock, C. Rodríguez-Rosario, T. Frauenheim, M. Paternostro, and K. Modi, *Phys. Rev. Lett.* **120**, 040405 (2018).
- [76] S. Milz, F. A. Pollock, and K. Modi, *Phys. Rev. A* **98**, 012108 (2018).
- [77] R. P. Feynman and F. L. Vernon, *Ann. Phys. (N. Y.)* **24**, 118 (1963).
- [78] F. Verstraete and J. I. Cirac, *Phys. Rev. B* **73**, 094423 (2006).
- [79] See Supplemental Material for details, which includes Refs. [80–82].
- [80] I. Sason, *Entropy* **20**, 896 (2018).
- [81] M. A. Nielsen and G. Vidal, *Quantum Inf. Comput.* **1**, 76 (2001).
- [82] M. A. Nielsen and I. L. Chuang, *Quantum Computation and Quantum Information* (Cambridge University Press, Cambridge, England, 2000).
- [83] S. Lorenzo, F. Ciccarello, and G. M. Palma, *Phys. Rev. A* **96**, 032107 (2017).
- [84] G. Vidal, *Phys. Rev. Lett.* **101**, 110501 (2008).
- [85] G. Evenbly and G. Vidal, *Phys. Rev. Lett.* **112**, 240502 (2014).
- [86] G. Carleo and M. Troyer, *Science* **355**, 602 (2017).
- [87] M. H. Amin, E. Andriyash, J. Rolfe, B. Kulchitsky, and R. Melko, *Phys. Rev. X* **8**, 021050 (2018).